Heliyon 10 (2024) e32607

Contents lists available at ScienceDirect

Heliyon

journal homepage: www.cell.com/heliyon

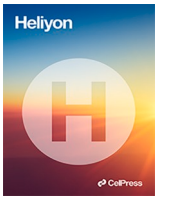

Research article

Draft genome sequences of two biocontrol agents isolated from the maize phyllosphere: *Bacillus subtilis* strain EM-A7 and *Bacillus velezensis* strain EM-A8

Aluminé Fessia [a,*], Melina Sartori [a], Julieta Orlando [b], Germán Barros [a], Andrea Nesci [a]

[a] *Laboratorio de Ecología Microbiana, Departamento de Microbiología e Inmunología, Facultad de Ciencias Exactas, Físico-Químicas y Naturales. Universidad Nacional de Río Cuarto, Ruta Nacional 36, Km 601, X5804ZAB Río Cuarto, Córdoba, Argentina. - Consejo Nacional de Investigaciones Científicas y Técnicas (CONICET), Argentina*

[b] *Laboratorio de Ecología Microbiana, Departamento de Ciencias Ecológicas, Facultad de Ciencias, Universidad de Chile, Las Palmeras 3425, Ñuñoa, Santiago, Chile*

ARTICLE INFO

Keywords:
Draft genome sequencing
Biofilm
Bacillus
Biocontrol agent
Phyllosphere

ABSTRACT

In the present study, the genomes of *B. subtilis* EM-A7 and *B. velezensis* EM-A8 were sequenced and annotated. The Illumina sequencing platform (NovaSeq PE150) was used to sequence the genomic DNA. There were 6 277 054 raw reads for EM-A7, with a Q20 of 97.52 % and 43.78 % GC, and 8 030 262 raw reads for EM-A8, with a Q20 of 97.53 % and 46.21 % GC. Annotation was carried out by the NCBI Prokaryotic Genome Annotation Pipeline (PGAP). The strains were classified taxonomically on the basis of an average nucleotide identity analysis (ANI), as well as through a dDDh analysis on the Genome-to-Genome Distance Calculator (GGDC v3.0). The pipeline predicted 4062 protein-coding sequences (CDSs) and 73 RNA genes (62 tRNA and 6 rRNA) for EM-A7, and 3797 protein-coding sequences (CDSs) and 80 RNA genes for EM-A8. These findings enhance our understanding of the two strains' potential as biocontrol agents to manage disease in maize.

1. Introduction

Stenberg et al. (2021) [1] define biological control as "… *the exploitation of living agents (including viruses) to combat pestilential organisms (pests and pathogens), directly or indirectly, for human good*". In other words, it is an approach that involves a pest, a biocontrol agent, and the humans that benefit from pest control. This strategy, which can minimize yield losses caused by crop disease, has the added advantage of being environmentally friendly: it prevents the emergence of pesticide resistance and does not pose the risks of traditional chemical control [1,2]. When isolated and introduced on leaves, epiphytic microorganisms can help plants antagonize pathogens from their ecosystem [3], i.e., they can act as biocontrol agents (BCAs). These microorganisms may impede pathogen growth directly, by outcompeting them for nutrients and space, interfering with their communication, parasitizing them, and/or secreting antimicrobial metabolites or enzymes. They may also inhibit pathogens indirectly, by triggering plant immune responses and modulating plant hormone levels [4].

* Corresponding author.
E-mail address: afessia@exa.unrc.edu.ar (A. Fessia).

https://doi.org/10.1016/j.heliyon.2024.e32607
Received 12 April 2024; Received in revised form 6 May 2024; Accepted 6 June 2024
Available online 13 June 2024

Maize (*Zea mays* L.), one of the main crops cultivated in Argentina, had an average annual yield of 32 million tons and occupied a 7.9 million ha planting area in 2022–2023 [5]. *Exserohilum turcicum* (Pass.) Leonard and Suggs (Syn. *Helminthosporium turcicum* Pass.), an important pathogen found on maize leaves, is the causal agent of the endemic disease known as Northern corn leaf blight (NCLB) [6]. It produces significant leaf lesions and can decrease yield by between 28 and 91 % [7].

Our laboratory tested 111 microbial isolates from the maize phyllosphere in terms of their ability to compete against *E. turcicum* [8]. This was done by observing how the isolates modified the growth parameters of the fungus. On the basis of those studies, two *Bacillus* spp. isolates (EM-A7 and EM-A8) were chosen, and their effectiveness in reducing the severity of NCLB was evaluated. They were found to be dominant at a distance (5/0), and when they interacted with the fungus on dual cultures, they decreased the pathogen's growth rate by about 84 and 98 % at water potential values (Ψ) of −1.38 MPa and −4.19 MPa [8]. In the greenhouse, both strains significantly reduced disease and symptom severity 20 and 39 days after initial inoculation. Under field conditions, they reduced the intensity of NCLB in maize plants (R2 to R4) by over 50 % over 40 days [9]. Further studies focused on their mode of action, which for BCAs generally involves enzymatic activity, the production of volatile organic compounds, and/or direct antibiosis mediated by other secondary metabolites [10]. The strains' tolerance to different environmental conditions was assessed as well. Phyllospheric microorganisms tend to be more tolerant to abiotic stresses such as oxidation, UV radiation, and desiccation, and are able to use nutrients and vitamins on the leaf surface for their own benefit [11–13]. EM-A7 and EM-A8 were tolerant to fluctuations in UV radiation, temperature, and osmotic stress, which suggests they are likely to have high survival rates on leaf surfaces.

The two *Bacillus* spp. isolates were subsequently identified at the genus level according to Berge's Manual of Systematic Bacteriology, and at the species level through biochemical and molecular methods, such as an API 50 CH kit (bioMérieux, Lyon, France) and sequencing of 16S–23S rRNA (Genbank accession number: OL704804-OL704805). This was complemented by matrix-assisted laser desorption/ionization-time of flight mass spectrometry (MALDI-TOF MS, Bruker Daltonik®, Bremen, Germany) [8,14].

Other experiments were then performed to look into the motility and ability of EM-A7 and EM-A8 to form biofilm. A biofilm is a three-dimensional structure or matrix made up of extracellular polymeric substances (EPSs). It facilitates colonization and survival on the leaf surface, and may promote either beneficial or harmful interactions with host plants, depending on the nature of the bacteria within it. We observed *in vitro* that biofilm formation and motility were modified in EM-A7 and EM-A8 by changing conditions of temperature, water potential, growth medium, and time [15]. More precisely, these conditions affected the robustness of their biofilm, as demonstrated by the morphological phenotypes of their colonies. As described in Fessia et al. [15], complex colonies were creamy and convex, had lobed irregular edges, and numerous wrinkles and veins spreading from the center to the edges. Less complex colonies were small, smooth, and round, with well-defined edges.

Given that light wavelength has been identified as a significant factor influencing the dynamics and functioning of leaf-associated microbes [16,17], we recently evaluated the multifaceted effects of light quality (i.e., wavelength and photosynthetically active photon flux density, or PPFD) on EM-A7 and EM-A8. Light quality was assayed in combination with water potential and nutrient availability. All these factors modified the behavior of the strains in terms of growth rate, formation of complex colonies and pellicles, *in vitro* biofilm quantification, motility, and antagonism toward *E. turcicum* [18]. The findings underscore the complexity of the interactions between the bacteria and environmental factors, and the importance of considering such factors when seeking to understand microbial dynamics and ecological relationships. In an effort to gain further insight into the potential of *B. subtilis* EM-A7 and *B. velezensis* EM-A8 as BCAs, the present study sequenced and annotated their draft genomes.

2. Methods

The strains were propagated in nutrient broth (NB) at 30 °C overnight, with 140 rpm agitation. A Wizard Genomic DNA Purification Kit (Promega, WI) was used to extract their genomic DNA, which was processed by Novogene (Durham, NC) as will be described next.

The DNA samples were quantitated with a Qubit fluorometer, and their integrity and purity was verified through gel electrophoresis. They were correctly qualified and the Illumina library was prepared. The genomic DNA was randomly sheared into short fragments, and these were end repaired, A-tailed, and further ligated with the Illumina adapter. Finally, they were sequenced through shotgun (SG) and paired-end (PE) strategies on the Illumina platform (NovaSeq PE150, Novogene).

There were 6 277 054 raw reads for EM-A7, with a Q20 of 97.52 % and 43.78 % GC, and 8 030 262 raw reads for EM-A8, with a Q20 of 97.53 % and 46.21 % GC. The quality report was read on FastQC (Galaxy Version 0.74+galaxy0) [19]. Adapters were trimmed and low-quality base reads were removed on Trimmomatic (Galaxy Version 0.38.1) [20], with quality being trimmed at a confidence level of Q30. These reads were used to obtain the genome sequence of each strain (herein referred to as draft genomes), which were *de novo* assembled into contigs and then scaffolded with SPAdes (Galaxy Version 3.15.4+galaxy1) on the UseGalaxy platform (https://usegalaxy.org/). Genome assembly quality was determined on QUAST (Galaxy Version 5.2.0+galaxy1), which provided detailed information about the contigs, such as the N50 length. The genomes were annotated using the NCBI Genome Automatic Annotation Pipeline (PGAP) by NCBI RefSeq, and their quality was analyzed by CheckM against a set of *Bacillus* marker genes. Functional annotation was made using the Kyoto Encyclopedia of Genes and Genomes database (KEGG) (https://www.genome.jp/kegg/) [21]. Reference genomes of *B. subtilis* and *B. velezensis* were compared with our sequences. These genomes were taken from the GenBank database (http://www.ncbi.nlm.nih.gov/genbank/) (accessed on November 22, 2023), and uploaded to the JSpecies software package (http://www.imedea.uib.es/jspecies) to calculate average nucleotide identity (ANI) using the default conditions. They were also put through the Genome-to-Genome Distance Calculator (GGDC v3.0) for a digital DNA-DNA hybridization (dDDH) analysis (https://ggdc.dsmz.de/) via the MASH algorithm, using the default conditions. *In silico* dDDH values were calculated on the Type (Strain) Genome Server (TYGS, available at https://tygs.dsmz.de/) using formula d_4. Gene clusters encoding the biosynthesis of secondary metabolites were identified, annotated and analyzed on antiSMASH version 6.1.1 via the UseGalaxy platform, using the default conditions [22].

The trees were made on TYGS, and the genome maps were built on Proksee (https://proksee.ca). Graphics were made on GraphPad Prism 5.0 (GraphPad Software, San Diego, CA).

3. Results and discussion

The whole genome shotgun (WGS) project for *B. subtilis* EM-A7 was deposited at GenBank under accession JAWLRH000000000.1 (BioProject: PRJNA1030342, BioSample: SAMN37905736). Its output consisted of 3 978 252 bp with an N50 length of 428.3 kb, and it predicted 89-fold genome coverage. The WGS project for *B. velezensis* EM-A8 was deposited at GenBank under accession JAWMQH000000000.1 (BioProject: PRJNA1030342, BioSample: SAMN37927805). Its output consisted of 3 963 136 bp with an N50 length of 337.1 kb, and it predicted 93-fold coverage. Annotation was performed by the NCBI Prokaryotic Genome Annotation Pipeline (PGAP).

The draft genome of each strain was assembled on SPAdes. For EM-A7, this resulted in 32 contigs and represented 89.73 % of the genome fraction with respect to a reference sequence. The longest contig was 700 711 bp, and the total length was 3 978 252 bp. The contamination level was 1 %, which is indicative of a high-quality assembly. Genome assembly and annotation completeness in terms of single-copy orthologs was assessed on BUSCO v. 5.4.6 [18], with bacilli_odb10 as the lineage dataset. Fully assembled single-copy orthologs (genome number = 302) constituted 99.7 % of the draft genome.

On the other hand, 210 contigs were obtained for EM-A7. The longest was 91 142 bp and the total length was 3 954 218 bp, which represented 90.14 % of the genome fraction in comparison with a reference sequence. The contamination level was also less than 1 % (high-quality assembly). Using the same software and dataset as for EM-A7, (BUSCO v. 5.4.6 and bacilli_odb10), we detected that 97.3 % of the EM-A8 genome featured complete and single-copy orthologs (number of genomes = 405), while 2.7 % was fragmented.

The GC content, which generally varies between 17 and 75 % from one organism to another, was about 44 % for EM-A7 and 46.5 % for EM-A8. These values are close to those corresponding to *B. subtilis* (44 %) and *B. velezensis* (48 %). Genome size was 4 Mb for both strains, in agreement with the values reported for *Bacillus* species [2,23].

An average nucleotide identity analysis (ANI) was carried out on the software JSpecies to classify EM-A7 and EM-A8 taxonomically. ANI values compare two genomic relatives at the nucleotide level, with a high degree of discrimination between closely related species: values $\geq$ 95 % have been set as the threshold to distinguish between species [2]. Whole genome sequences of different strains of *Bacillus* spp. were downloaded from GenBank and compared against the draft genomes of our two strains. The analysis indicated a close relationship between them, with the ANI value for EM-A7 being $\geq$97.97 %, and that for EM-A8 between 97.26 and 98.81 % (Table 1).

Further comparison with reference *Bacillus* spp. strains was made through a dDDH analysis on the Genome-to-Genome Distance Calculator (v3.0). With dDDH values $\geq$ 90.60 % (Table 1), the sequence of EM-A7 was highly similar to the sequences of *B. subtilis* strains, and that of EM-A8 was highly similar to those belonging to *B. velezensis* strains (Fig. 1).

Fig. 2 shows the genome map of EM-A7 (2A) and EM-A8 (2B). All the predicted genes were annotated and calculated on the PGAP pipeline with *B. subtilis* or *B. velezensis* CheckM marker sets. In the case of EM-A7, 4062 protein-coding sequences (CDSs) and 68 RNA genes (62 tRNA and 6 rRNA) were predicted (Fig. 3). When this genome was aligned with sequences from databases such as RAST-KEGG, 4185 coding sequences and 74 RNAs were identified. As seen in Fig. 3, the most prevalent subsystem categories encoded by these genes are amino acids and their derivatives, carbohydrates, cofactors, vitamins, pigments and protein metabolism. In terms of relative importance, the most relevant functional category is amino acid derivatives and carbohydrate metabolism (31.67 %, 530/1643 genes). An important percentage of genes (8.60 %, 144/1643) is implicated in the synthesis of cofactors, vitamins, prosthetic

Table 1
Comparative genomic analysis of *Bacillus subtilis* EM-A7 *and Bacillus velezensis* EM-A8 with the genomes of another *Bacillus* spp.

Strain	GenBank Accession N° assembly	ANI (%)	dDDH (%)	GC (%)	Size (bp)
Bacillus subtilis EM-A7	ASM3394932v1	–	–	44.00	3 978 252
B. subtilis SG6s	ASM78283v1	98.56	94.20	43.82	4 079 669
B. subtilis PS832	ASM78929v1	99.88	92.20	43.52	4 215 367
B. subtilis NCIB 3610	ASM205596v1	99.99	90.60	43.34	4 299 822
B. subtilis DSM 10	ASM2953741v1	99.99	90.60	43.35	4 299 854
B. subtilis UD1022	ASM101509v1	97.97	98.99	43.89	4 025 326
B. subtilis BS49	GCF_000953615.1	99.96	91.50	43.47	4 251 652
Bacillus velezensis EM-A8	ASM3394937v1	–	–	46.50	3 963 136
B. velezensis FZB42	ASM1578v2	98.57	92.10	46.48	3 918 589
B. velezensis CAU B046	ASM28369v1	97.26	93.30	46.51	4 019 861
B. velezensis AS43.3	ASM31947v1	98.81	94.60	46.59	3 961 368
B. velezensis JS25R	ASM76955v1	97.84	90.60	46.39	4 014 440
B. velezensis G341	ASM102359v1	98.28	92.00	46.49	4 009 746
B. velezensis YJ11-1-4	ASM31947v1	97.86	94.60	46.42	4 006 637

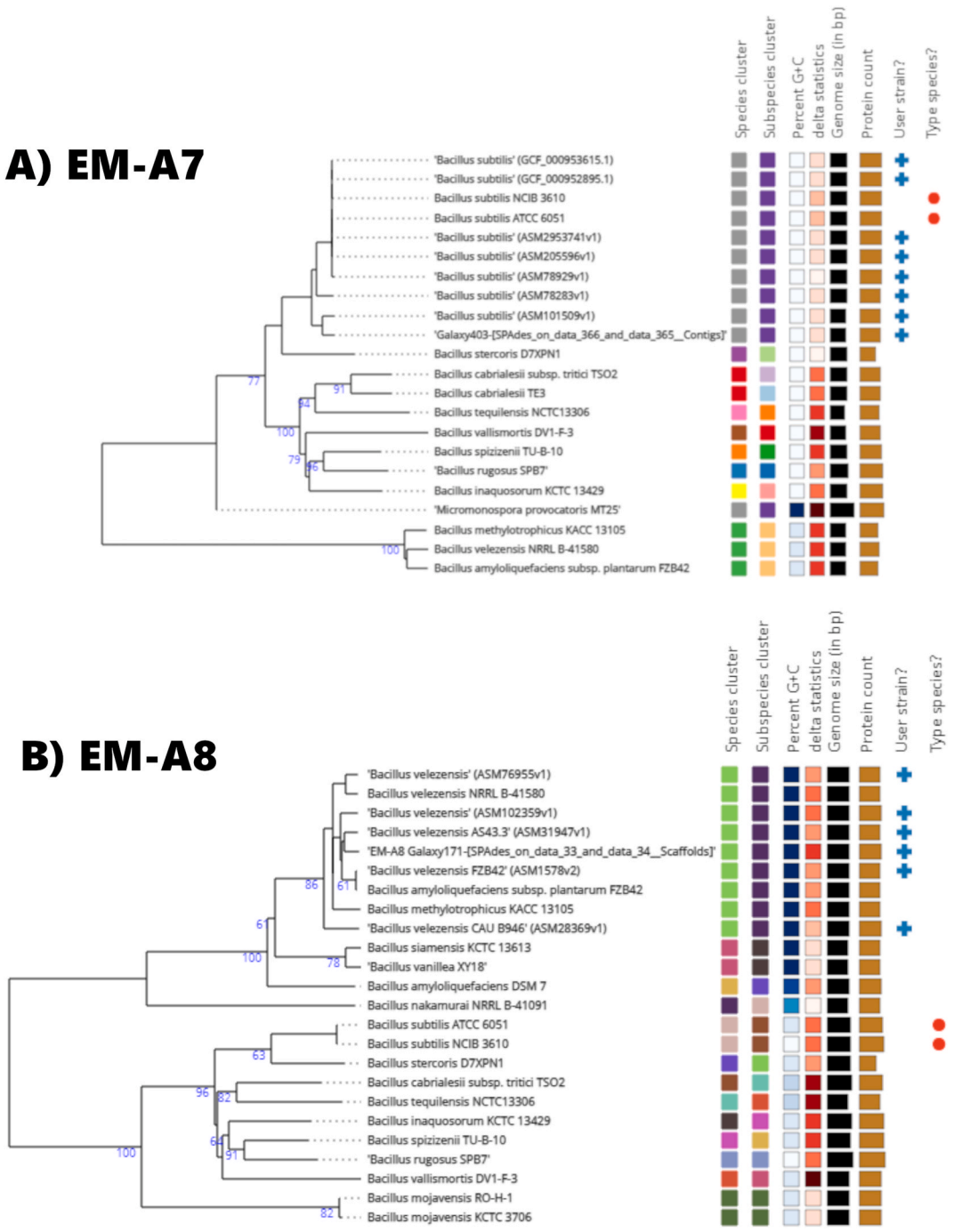

Fig. 1. GBDP tree (whole-genome, sequence-based). Tree inferred with FastME 2.1.6.1 [49] from GBDP distances calculated from genome sequences. The branch lengths are scaled in terms of the GBDP distance formula d5. The numbers above the branches are GBDP pseudo-bootstrap support values > 60 % from 100 replications, with an average branch support of 47.8 %. (A) *Bacillus subtilis* EM-A7 (B) *Bacillus velezensis* EM-A8. The trees were made using Type (Strain) Genome Server (TYGS), a free bioinformatic platform available at https://tygs.dsmz.de.

groups and pigments, most of which are essential in diverse metabolic pathways. A minor percentage (5.2 %, 87/1643 genes) is associated with the metabolism of aromatic compounds, nitrogen, potassium, phosphorus, iron and sulfur. Furthermore, there are genes related to dormancy and sporulation (5.85 %, 98/1643), the stress response (2.80 %, 47/1643), motility and chemotaxis (2.69 %, 45/1643), and secondary metabolism (0.35 %, 6/1643).

For EM-A8, 3797 protein-coding sequences (CDSs) and 80 RNA genes were predicted (Fig. 3). According to the KEGG database, the

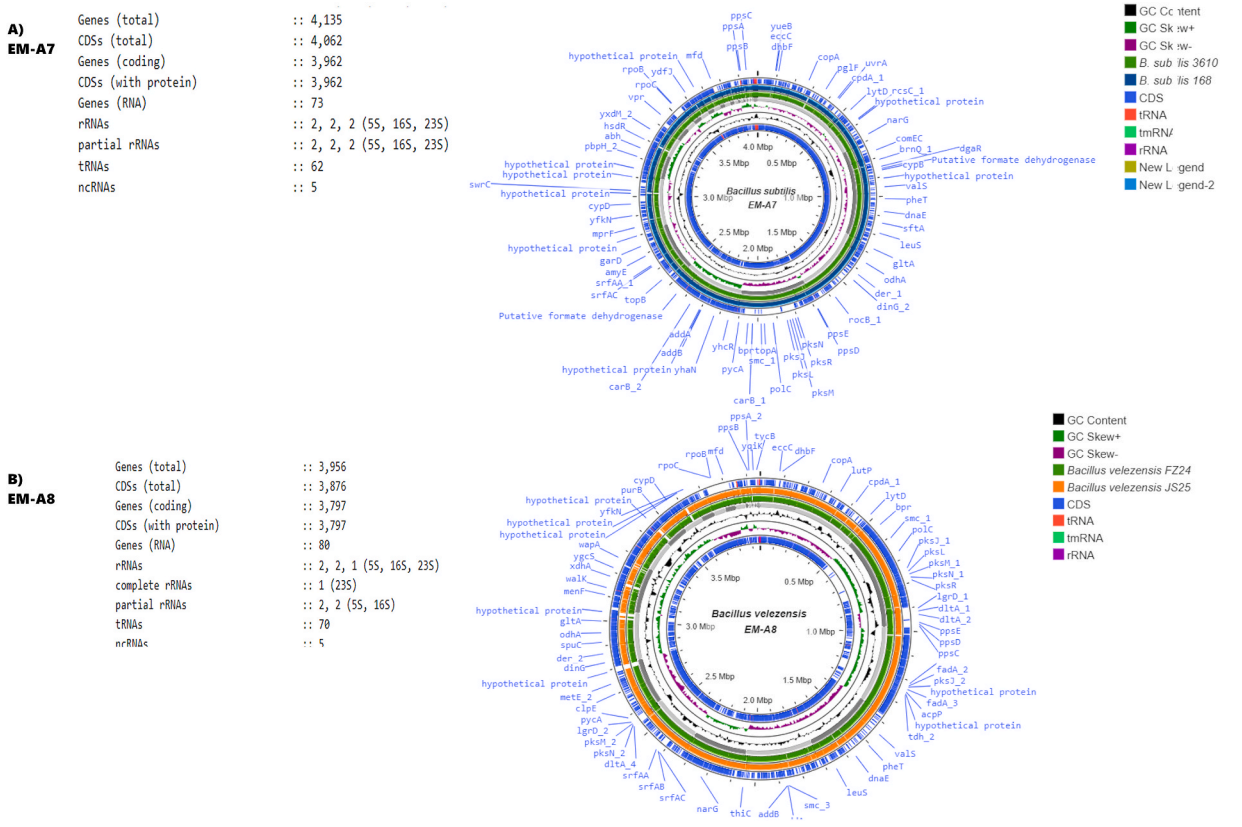

Fig. 2. Whole genome information and genome map of *Bacillus subtilis* EM-A7 (A) and *Bacillus velezensis* EM-A8 (B). The circles (outer to inner) represent rRNA, tmRNA, tRNA, nomenclature and locations of CDDs, comparative sequence with related strains, GC skew and GC content. The circles were mapped using Proksee (https://proksee.ca).

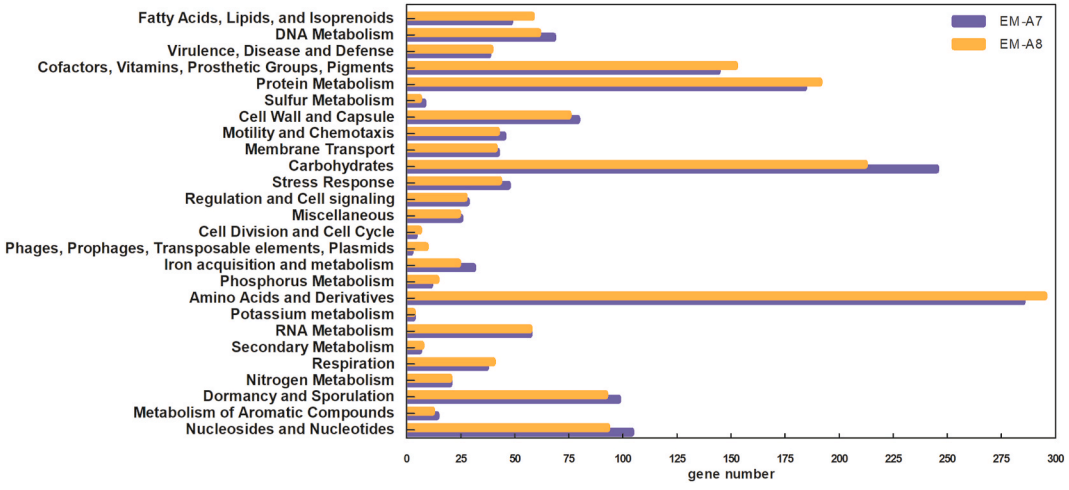

Fig. 3. Number of genes per category.

distribution of genes across functional subsystem categories is similar to that of EM-A7 genes (Fig. 3). The most prevalent categories are amino acids and derivatives (17.95 %), carbohydrates (12.90 %), and cofactors, vitamins, pigments and protein metabolism (9.25 %). These results are similar to those reported previously [2,23–25].

Table 2 shows representative genes in EM-A7 and EM-A8 which are related to biofilm, motility, plant growth promotion and the synthesis of resistance inducers. These genes have been reported in *Bacillus* spp. by several authors before [2,23–25]. Furthermore,

Table 2
Representative genes of *Bacillus subtilis* EM-A7 and *Bacillus velezensis* EM-A8 related to biofilm, motility, promotion of plant growth/defenses, and synthesis of resistance inducers.

Gene	Annotation		Protein	Function
	EM-A7	EM-A8		
abrB	R3M60_19295	R5D67_19070	Transition state regulator	Transcription control of biofilm
*als*S	R3M60_02665	R5D67_11345	Acetolactate synthase	Plant resistance type ISR
*apr*E	R3M60_11540	absent	Subtilisin E	Degradation of proteins, N source
*aro*B	R3M60_07695	R5D67_06185	3-dehydroquinate synthase	Plant growth promotion, Indole-3-acetic acid biosynthesis
*aro*C	R3M60_07700	R5D67_06180	Chorismate synthase	Plant growth promotion, Indole-3-acetic acid biosynthesis
*aro*H	R3M60_07690	R5D67_06190	Chorismate mutase	Plant growth promotion, Indole-3-acetic acid biosynthesis
*bgl*C	R3M60_13550	absent	6-phospho-beta-glucosidase	Carbohydrate catabolic process
*bsl*A	R3M60_00050	R5D67_00005	Hydrophobic protein	Biofilm assembly factor
comA	R3M60_00380	absent	Two-component response regulator	Positive regulation of late competence genes and surfactin production
*com*X	R3M60_00390	R5D67_00320	Competence pheromone	Quorum-sensing pheromone for development of genetic competence
*cor*A	R3M60_14760	R5D67_18415	Magnesium/cobalt transporter CorA	Plant growth promotion, Magnesium utilization
dacA	R3M60_20270	R5D67_19455	Carboxypeptidase	Plant resistance type PTI
Ecs	R3M60_11410	R5D67_09215	ABC transporter ATP-binding protein EcsA	Control of protein secretion
Efp	R3M60_08610	R5D67_05205	Similar to elongation factor P	Swarming motility
Epr	R3M60_17670	absent	Extracellular protease	Degradation of proteins, minor protease, N source
*eps*A-O	R3M60_01815	R5D67_01740	Operon for exopolysaccharide biosynthesis	Assembly of extracellular matrix
*flg*K	R3M60_02335	R5D67_02250	Flagellar hook-associated protein	Elicitation of plant basal defense
flgL	R3M60_02330	R5D67_02245	Flagellin	Plant resistance type PTI
fliD	R3M60_02300	absent	Flagellar capping protein	Elicitation of plant basal defense
Fni	R3M60_07790	R5D67_06100	Isopentenyl-diphosphate Delta-isomerase	Plant resistance type ISR
gale	R3M60_18180	R5D67_08265	UDP-glucose 4-epimerase GalE	Carbohydrate metabolism
*gal*T	R3M60_17555	R5D67_08270	UDP-glucose-hexose-1-phosphate uridylyltransferase	Carbohydrate metabolism
Hag	R3M60_02310	R5D67_02225	Flagellin	Bacterial type-flagellin
*ilv*B	R3M60_05025	R5D67_06765	Acetolactate synthase 3 catalytic subunit	Plant resistance type ISR, plant growth promotion
*ilv*N	R3M60_05020	R5D67_06760	Acetolactate synthase small subunit	Plant resistance type ISR: plant growth promotion
*isp*D	R3M60_18050	R5D67_18795	2-C-methyl-D-erythritol 4-phosphate	Plant resistance type ISR
*isp*E	R3M60_19250	R5D67_19025	4-diphosphocytidyl-2-C-methyl-D-erythritol kinase	Plant resistance type ISR
ispF	R3M60_18045	R5D67_18790	2-C-methyl-D-erythritol 2,4-cyclodiphosphate synthase	Plant resistance type ISR
*ktr*C	R3M60_16540	R5D67_12635	Ktr system potassium transporter KtrC	Plant growth promotion, Potassium transporter
lytS	R3M60_05340	absent	Sensor histidine kinase controlling autolysis	Transcription control of biofilm formation
*met*C	R3M60_12360	R5D67_08365	Cystathionine beta-lyase	Plant resistance type ISR
*met*E	R3M60_15850	R5D67_13245	5-methyltetrahydropteroyltriglutamate–homocysteine S-methyltransferase	Plant resistance type ISR
*mgt*E	R3M60_15915	R5D67_13205	Magnesium transporter	Plant growth promotion, Magnesium utilization
*mmu*M	R3M60_14090	R5D67_12200	Homocysteine S-methyltransferase	Plant resistance type ISR
*moa*A	R3M60_03035	R5D67_11030	Molybdenum cofactor biosynthesis protein A	Cofactor for nitrogen assimilation
Mpr	R3M60_14170	R5D67_18270	Extracellular metalloprotease	Degradation of proteins, minor protease, N source
*nar*H	R3M60_03335	R5D67_10750	Nitrate reductase subunit beta	Plant growth promotion, Nitrate transport and reduction
*nar*I	R3M60_03325	R5D67_10760	Nitrate reductase subunit gamma	Plant growth promotion, Nitrate transport and reduction
narJ	R3M60_03330	R5D67_10755	Nitrate reductase molybdenum cofactor assembly chaperone	Plant growth promotion, Nitrate transport and reduction
*nar*K	R3M60_03360	R5D67_10725	Nitrate transporter NarK	Plant growth promotion, Nitrate transport and reduction
*nas*D	R3M60_13630	R5D67_11835	NADPH-nitrite reductase	Plant growth promotion, Potassium transporter
*nir*D	R3M60_13635	R5D67_11840	Nitrite reductase small subunit NirD	Plant growth promotion, Nitrate transport and reduction
*pel*A	R3M60_14975	absent	Pectate lyase	Degradation of pectin, C source
*pgs*ABC	R3M60_02600	R5D67_03475	Operon for poly-gamma glutamic acid biosynthesis	Adherence of charged molecules during biofilm formation
*phr*A	R3M60_12660	R5D67_13650	Phosphatase rapA inhibitor	Secreted regulator of the activity of phosphatase RapA

(*continued on next page*)

Table 2 (*continued*)

Gene	Annotation		Protein	Function
	EM-A7	EM-A8		
*phr*C	R3M60_13370	absent	Phosphatase rapC inhibitor	Secreted regulator of the activity of phosphatase RapC
*phr*K	absent	R5D67_14200	Phosphatase rapK inhibitor	Secreted regulator of the activity of phosphatase RapK
*phy*C	R3M60_07145	R5D67_14240	phytase	3-phytase activity
*pst*A	R3M60_03495	R5D67_04960	Phosphate ABC transporter permease	Plant growth promotion, Phosphate solubilization
*pst*B	R3M60_03490	R5D67_04965	Phosphate ABC transporter ATP-binding protein PstB	Plant growth promotion, Phosphate solubilization
pstc	R3M60_03500	R5D67_04955	Phosphate ABC transporter permease subunit	Plant growth promotion, Phosphate solubilization
*rap*A	R3M60_12655	absent	Response regulator aspartate phosphatase A	Negative regulation of Spo0F
*rap*B	R3M60_03030	absent	Response regulator aspartate phosphatase B	Negative regulation of Spo0F
*rap*D	R3M60_02860	absent	Response regulator aspartate phosphatase D	Regulation of coma regulon
*rap*H	R3M60_15325	absent	Response regulator aspartate phosphatase H	Negative regulation of coma
*rap*J	R3M60_13870	absent	Response regulator aspartate phosphatase J	Control of expression of genes regulated by Spo0A
*res*E	R3M60_07905	absent	Sensor histidine kinase	Control of aerobic and anaerobic respiration
*sac*B	R3M60_01860	absent	Levansucrase	Synthesis of levan
sigH	R3M60_18010	R5D67_18755	Sigma factor H	Initial stage of biofilm
sigW	R3M60_14380	R5D67_19255	Sigma factor W	Transcription control of biofilm
*sin*I	R3M60_08685	R5D67_10230	Antagonist of sinR	Transcription control of biofilm formation
*sin*R	R3M60_08690	R5D67_05130	Master regulator	Transcription control of biofilm formation
*sip*W	R3M60_08700	absent	Type I signal peptidase	Involved in processing of TasA and TapA
spo0A	R3M60_08495	R5D67_05320	Master regulator of initiation of sporulation	Sporulation, biofilm
*srf*ABCD	R3M60_13515	R5D67_11765	surfactin non-ribosomal peptide synthetase	Sporulation, antibiotic biosynthetic process
swrA	R3M60_02240	R5D67_02155	Swarming motility protein	Swarming motility
*tap*A	R3M60_08705	R5D67_05115	Auxilliar protein	Assembly and anchoring of TasA fibers
*tas*A	R3M60_08695	R5D67_05125	Amyloid-like protein	Amyloid-like fibers in extracellular matrix
*trp*A	R3M60_07660	R5D67_06220	Tryptophan synthase subunit alpha	Plant growth promotion, Indole-3-acetic acid biosynthesis
*trp*C	R3M60_07675	R5D67_06205	Indole-3-glycerol phosphate synthase	Plant growth promotion, Indole-3-acetic acid biosynthesis
*trp*D	R3M60_07680	R5D67_06200	Anthranilate phosphoribosyltransferase	Plant growth promotion, Indole-3-acetic acid biosynthesis
*trp*E	R3M60_07685	R5D67_06195	Anthranilate synthase component I	Plant growth promotion, Indole-3-acetic acid biosynthesis
trps	R3M60_12110	R5D67_08625	Tryptophan–tRNA ligase	Plant growth promotion, Indole-3-acetic acid biosynthesis
tuf	R3M60_17935	R5D67_18680	Elongation factor Tu	Plant resistance type PTI
vpr	R3M60_17505	absent	Extracellular protease	Degradation of proteins, minor protease, N source
*xyn*A	R3M60_06670	R5D67_11070	Endo-1,4-beta-xylanase	Degradation of xylan, C source
*xyn*B	R3M60_09300	R5D67_03790	Glycoside hydrolase	Carbohydrate metabolism
*xyn*C	R3M60_08965	absent	Glucuronoxylanase	Degradation of xylan, C source
yczE	R3M60_13475	absent	Integral membrane protein	Surface motility and biofilm
*ydb*K	R3M60_12955	absent	Hypothetical protein	Transcription control of biofilm formation

they have been linked to an increased potential to adapt to changing environmental conditions on plant surfaces [23,26]. The presence of genes that encode the synthesis of enzymes like hydrolase, protease, glycoside hydrolase or glucuronoxylanase suggests that both strains could use carbon sources available in plant surface exudates, e.g., xylan or pectin. Previously, we detected that EM-A7 and EM-A8 were able to produce hydrolytic enzymes such as chitinase, protease and β-1,3-glucanase *in vitro* [10]. The latter is responsible for the lysis and degradation of the cell and sclerotium wall in fungi [10], and could thus work as a mechanism of biocontrol. The synthesis of sulfur and iron, which is also encoded by genes in these two draft genomes, could be ecologically advantageous to bacteria and plant health, since the mobilization and bioavailability of micronutrients is important for plant development [27].

On the other hand, the genome of EM-A7 (but not that of EM-A8) contains a gene encoding the ABC transporter of bacitracin, an antibiotic. This may provide EM-A7 with immunity to bacitracin and its related metabolites [23,28,29], and thus enhance the effectiveness and persistence of the strain as a BCA.

Several genes in the two draft genomes are related to motility and chemotaxis. This is especially important, since BCAs can only protect plants effectively if they succeed in establishing themselves in the host plant through chemotaxis, motility, and appropriate growth [30]. Chemotaxis allows bacteria to swarm across solid surfaces such as leaves and colonize them [31]. Under different environmental conditions (nutrient agar and different LED lights), EM-A7 and EM-A8 were able to swim and swarm [15,32]. Their genomes include genes *efp* (similar to elongation factor P), *hag* (flagellin), *swrA* (swarming motility protein) and *yczE* (integral membrane protein).

Other genes that were identified in the two strains are associated with biofilm formation. On leaf surfaces, biofilm awards microorganisms protection against numerous adverse conditions, and helps cells to become attached [33]. Attachment to a surface makes it possible to form communities in which each cell can obtain additional benefits from its neighbor's phenotypic versatility [14]. In BCAs, the diversification of cell types in biofilms suggests that this lifestyle enables them to better adapt to and resist hostile conditions in agricultural ecosystems. EM-A7 and EM-A8 have several genes implicated in the assembly and regulation of biofilm formation, such as genes that encode the synthesis of components of the extracellular matrix. Gene *bslA* encodes a hydrophobic protein which confers hydrophobicity and contributes to biofilm architecture. Operon *pgs*B synthesizes polygamma glutamic acid, which facilitates the adherence of molecules during biofilm formation. Operon *eps*A-O encodes the synthesis of exopolysaccharides, and operon *tapA* that of amyloid fibers and signal peptidase. The TasA protein encoded by *tasA* is a structural protein of the extracellular matrix and major protein component of fibers. Finally, gene *srf*A is related to surfactin, a lipopeptide component of biofilm which acts as a surfactant and has antimicrobial activity [28,34,35].

In addition, we found regulatory genes such as *lytS,* a sensor histidine kinase controlling autolysis; *sig*H-W, a sigma factor H and W related with the transcriptional control of biofilm; *sip*W, a signal peptidase W, which processes TapA and TasA, and activates the expression of *eps*; *sin*R, which encodes a master regulator; *sir*R-*sin*I, an epigenetic switch that controls biofilm formation and the spo0A pathway, and which is also a main transcriptional regulator involved in the control of genes behind matrix expression and sporulation [35,36].

Quorum sensing (QS) is a process through which bacterial cells communicate with each other to coordinate activities such as biofilm formation, interactions with the plant, and other physiological responses. Operon *comQXPA* in *Bacillus* spp. is a QS system that controls the expression of several genes involved in the competition against other microorganisms or the production of surfactin, among other genes [37]. DegSU is a two-component system related to signal transduction in response to environmental stimuli. The genes for *comQXPA* and *DegS*U were found in EM-A7 and EM-A8, although the former was incomplete. Similar results were described by Na et al. (2023) [38].

In *Bacillus* spp., extracellular Phr peptides are implicated in relevant processes such as the synthesis of antibiotics, sporulation, and biofilm formation. Nine genes in EM-A7 encode Rap proteins (RapA to RapG) and five Phr peptides (PhrA to PhrG). These proteins inhibit the response regulators of different two-component regulatory systems [39]. Genes associated with these regulatory systems were not found in EM-A8.

On the other hand, the analyses revealed that both draft genomes include genes implicated in the synthesis of molecules known as elicitors. As their name indicates, these elicit or induce nonspecific basal plant immunity or induced systemic resistance (ISR), and can

Table 3
Putative gene clusters that encode secondary metabolites in *B. subtilis* EM-A7 and *B. velezensis* EM-A8.

Cluster	Type	Most similar known clusrer	MIBiG (% of genes that show similarity)	Bioactivity
B. subtilis EM-A7				
Cluster 1	NRPS	Bacillibactin NRP	BGC0000309 (100 %)	Iron-acquisition and antibacterial
Cluster 2	Sactipeptide	Subtilosin A – RiPP thiopeptide	BGC0000602 (100 %)	–
Cluster 3	Other	Bacilysin – other	BGC0001184 (100 %)	Antibacterial
Cluster 4	NRPS	Plipastatin – NRP	BGC0000407 (30 %)	–
Cluster 5	Terpene	–	–	–
Cluster 6	T3PKS	–	–	–
Cluster 7	NRPS-beta lactone	Fengycin – NRP	BGC0001095 (73 %)	Antibacterial and antifungal
Cluster 8	NRPS- transAT-PKS	Bacillaene – polyketide + NRP	BGC0001089 (100 %)	Antibacterial and antifungal
Cluster 9	T3PKS-PKS like	–	–	–
Cluster 10	NRPS	Surfactin – NRP lipopeptide	BGC0000433 (82 %)	Antibacterial
Cluster 11	NRPS	Plipastin – NRP	BGC0000407 (30 %)	Antifungal
Cluster 12	NRPS	Plipastin – NRP	BGC0000407 (15 %)	Antifungal
B. velezensis EM-A8				
Cluster 1	NRPS – RIPP- like	Bacillibactin NRP	BGC0000309 (100 %)	Iron acquisition and antibacterial
Cluster 2	TransAT-PKS – T3PKS – NRPS	Bacillaene - polyketide + NRP	BGC0001089 (100 %)	Antibacterial and antifungal
Cluster 3	NRPS - TransAT-PKS – Beta lactone	Fengycin – NRP	BGC0001095 (86 %)	Antibacterial and antifungal
Cluster 4	TransAT-PKS	Difficidin - polyketide + NRP	BGC0000176 (100 %)	Antibacterial
Cluster 5	Terpene	–	–	
Cluster 6	Other	Bacilysin – other	AP012495_c1 (100 %)	Antibacterial
Cluster 7	NRPS	Surfactin – NRP – lipopeptide	BGC0000433 (91 %)	Antibacterial
Cluster 8	T3PKS	–	–	–
Cluster 9	Terpene	–	–	–
Cluster 10	NRPS	Rhizocticin A – other	BGC0000926 (16 %)	–
Cluster 11	NRPS	Fengycin – NRP	BGC0001095 (20 %)	Antibacterial and antifungal
Cluster 12	NRPS	Plipastin – NRP	BGC0000407 (30 %)	Antifungal
Cluster 13	NRPS	–	–	–

therefore enhance the plant's resistance to pathogens [40]. An example of such elicitors are flagellin proteins, which are also essential for motility, and which are encoded by genes *flgK*, *flgL* and *fliD* in EM-A7 and EM-A8. Besides, *tufA* genes encoding an elongation factor were detected [23].

Other gene clusters found in the genomes of both strains are related to the promotion of plant growth. Essential elements such as nitrogen, phosphorus, and potassium play crucial roles in plant growth and development, and several genes in EM-A7 and EM-A8 may allow the bacteria to make such elements more readily available for the plant. Genes *nar* (H–K), *nas*D, and *nir*D have been predicted to be involved in nitrate transport and reduction; *pst* (ABC), a three-gene cluster, is involved in phosphate solubilization; and *KtrC* and *yug*O are implicated in potassium uptake [2].

Finally, the antiSMASH analysis showed that EM-A7 and EM-A8 feature 12 and 9 putative gene clusters, respectively, which encode the synthesis of secondary metabolites with antagonistic characteristics (Table 3). *Bacillus* isolates have exhibited different modes of antagonistic action, e.g. enzymatic activity, the production of volatile organic compounds, and/or direct antibiosis through other secondary metabolites [14]. The genomes of the two strains studied here contain genes encoding the synthesis of non-ribosomal peptide synthetases (NRPSs) and polyketide synthetases (PKSs), as well as ribosomally synthesized clusters. NRPSs have been associated with the synthesis of bacillibactin, subtilisin, bacilysin, pliplastin, fengycin, and surfactin, all of which have antimicrobial properties. Fengycin and surfactin, in particular, are cyclic lipopeptides that can not only suppress pathogenic bacteria and fungi that affect plants, but also induce ISR [41]. Mo reover, they may confer an advantage to *Bacillus* strains in ecological niches [42]. EM-A8 also has genes encoding difficidin, bacillaene, and butirosin A/butirosin B, which have antibacterial and antifungal effects [43–46]. In general, these findings support those of a previous in vitro study in which the two strains demonstrated a strong production of volatile compounds and antibiotics [10].

In summary, the draft genomes sequenced here for EM-A7 and EM-A8 have a similar size and are of appropriate quality according to the BUSCO values. EM-A7 has a greater number of protein-coding sequences than EM-A8 (4062 vs 3797). The distribution of genes across functional categories is similar in both strains, with a significant percentage of genes involved in the metabolism of amino acid derivatives and carbohydrates. Several genes found in EM-A7 were not present in EM-A8, e.g. genes associated with two-component response regulators and degradation enzymes, and genes encoding compound degradation, surface motility and control of biofilm formation. However, both draft genomes include genes related to colonization, biofilm formation, motility, and the production of secondary metabolites with antimicrobial characteristics. These may favor the establishment and activity of EM-A7 and EM-A8 as BCAs on the leaf surface of maize.

4. Conclusion

The bioinformatics analyses reported here resulted in the obtention of the draft genome sequences for *B. subtilis* EM-A7 and *B. velezens*is EM-A8. These strains, which were isolated from the maize phyllosphere, had been previously studied *in vitro*, in the greenhouse and in the field, and repeatedly showed promising biocontrol potential against a pathogen affecting maize. Knowledge about the genes that encode their antimicrobial activity and those properties that may favor their survival on maize leaves can help us have a greater understanding of their possible applications as biocontrol agents, as well as of the complex interactions between biocontrol agents, pathogens, and the environment.

Funding statement

The experimental assays were supported by grants from SECyT-UNRC PPI 2020–2022 (Res. 357/20), Consejo Nacional de Investigaciones Cientificas y Tecnicas (CONICET, PIP 11220210100161CO), and Agencia Nacional de Promoción Científica y Tecnológica (PICT 2018–04220 and PICT 2021-00455).

Ethical approval

No studies with human participants or animals were performed as part of the research described in this article.

Consent to publish

All the authors agree to the publication of the article.

Statement of informed consent

The research does not involve human participants or experiments with animals.

Data availability statement

The datasets in this study can be found in online repositories. The draft genome of *B. subtilis* EM-A7 was deposited in NCBI GenBank under accession JAWLRH000000000.1. The draft genome of *B. velezensis* EM-A7 was deposited in NCBI GenBank under accession JAWMQH000000000.1.

CRediT authorship contribution statement

Aluminé Fessia: Writing – review & editing, Writing – original draft, Methodology, Funding acquisition, Formal analysis, Data curation, Conceptualization. **Melina Sartori:** Writing – review & editing, Investigation, Conceptualization. **Julieta Orlando:** Writing – review & editing, Conceptualization. **Germán Barros:** Writing – review & editing, Funding acquisition, Conceptualization. **Andrea Nesci:** Writing – review & editing, Writing – original draft, Supervision, Investigation, Funding acquisition, Formal analysis, Conceptualization.

Declaration of competing interest

The authors declare that they have no known competing financial interests or personal relationships that could have appeared to influence the work reported in this paper.

References

[1] J.A. Stenberg, I. Sundh, P.G. Becher, et al., When is it biological control? A framework of definitions, mechanisms, and classifications, J. Pest. Sci. 94 (2021) 665–676, https://doi.org/10.1007/s10340-021-01354-7.

[2] L. Xie, L. Liu, Y. Luo, X. Rao, Y. Di, H. Liu, F. Li, Complete genome sequence of biocontrol strain *Bacillus velezensis* YC89 and its biocontrol potential against sugarcane red rot, Front. Microbiol. 14 (2023) 1180474. https://10.3389/fmicb.2023.1180474.

[3] I. Bashir, A.F. War, I. Rafiq, Z.A. Reshi, I. Rashid, Y.S. Shouche, Phyllosphere microbiome: Diversity and functions, Microbiol. Res. 254 (2022) 126888, https://doi.org/10.1016/J.MICRES.2021.126888.

[4] M. Legein, W. Smets, D. Vandenheuvel, T. Eilers, B. Muyshondt, E. Prinsen, S. Lebeer, Modes of action of microbial biocontrol in the phyllosphere, Front. Microbiol. 11 (2020) 1619, https://doi.org/10.3389/fmicb.2020.01619.

[5] Bolsa de Comercio de Rosario (BCR), 2023. Available in, https://www.bcr.com.ar/es/buscar/es-mercados-gea-estimaciones-nacionales-de-produccion-estimaciones-2023.

[6] B.L. Navarro, L. Ramos Romero, M.B. Kistner, J. Iglesias, A. von Tiedemann, Assessment of physiological races of Exserohilum turcicum isolates from maize in Argentina and Brazil, Trop. Plant Pathol 46 (2021) 371–380, https://doi.org/10.1007/S40858-020-00417-X/.

[7] T.R. Reddy, P.N. Reddy, R.R. Reddy, S.S. Reddy, Management of turcicum leaf blight of maize caused by Exserohilum turcicum in maize, International Journal of Scientific and Research Publications 3 (2013) 1–4.

[8] M. Sartori, A. Nesci, A. Formento, M. Etcheverry, Selection of potential biological control of Exserohilum turcicum with epiphytic microorganisms from maize, Rev. Argent. Microbiol. 47 (2015) 62–71, https://doi.org/10.1016/j.ram.2015.01.002.

[9] M. Sartori, A. Nesci, J. García, M.A. Passone, A. Montemarani, M. Etcheverry, Efficacy of epiphytic bacteria to prevent northern leaf blight caused by Exserohilum turcicum in maize, Rev. Argent. Microbiol. 49 (2017) 75–82, https://doi.org/10.1016/j.ram.2016.09.008.

[10] M. Sartori, M. Bonacci, P. Barra, A. Fessia, M. Etcheverry, A. Nesci, G. Barros, Studies on possible modes of action and tolerance to environmental stress conditions of different biocontrol agents of foliar diseases in maize, Agric. Sci. 11 (2020) 552–566, https://doi.org/10.4236/as.2020.116035.

[11] J.A. Vorholt, Microbial life in the phyllosphere, Nat. Rev. Microbiol. (2012), https://doi.org/10.1038/nrmicro2910.

[12] S. Yoshida, M. Koitabashi, D. Yaginuma, M. Anzai, M. Fukuda, Potential of bioinsecticidal *Bacillus thuringiensis* inoculum to suppress gray mold in tomato based on induced systemic resistance, J. Phytopathol. 167 (11–12) (2019) 679–685, https://doi.org/10.1111/jph.12864.

[13] V. Chaudhry, P. Runge, P. Sengupta, G. Doehlemann, J.E. Parker, E. Kemen, Shaping the leaf microbiota: plant–microbe– microbe interactions, J. Exp. Bot. 72 (1) (2021) 36–56, https://doi.org/10.1093/jxb/eraa417.

[14] A. Fessia, P. Barra, G. Barros, A. Nesci, Could *Bacillus* biofilms enhance the effectivity of biocontrol strategies in the phyllosphere? J. Appl. Microbiol. 133 (2022) 2148–2166, https://doi.org/10.1111/JAM.15596.

[15] A. Fessia, M. Sartori, D. García, L. Fernández, R. Ponzio, G. Barros, A. Nesci, *In vitro* studies of biofilm-forming *Bacillus* strains, biocontrol agents isolated from the maize phyllosphere, Biofilm 4 (2022) 100097, https://doi.org/10.1016/J.BIOFLM.2022.100097.

[16] B.W. Alsanius, L. Vaas, S. Gharaie, M.E. Karlsson, A.K. Rosberg, W. Wohanka, S. Khalil, S. Windstam, Dining in blue light impairs the appetite of some leaf epiphytes, Front. Microbiol. 12 (2021) 725021, https://doi.org/10.3389/FMICB.2021.725021/BIBTEX.

[17] B.W. Alsanius, M. Karlsson, A.K. Rosberg, M. Dorais, M.T. Naznin, S. Khalil, K.J. Bergstrand, Light and microbial lifestyle: the impact of light quality on plant–microbe interactions in horticultural production systems—a review, Horticulturae 5 (2019) 1–24, https://doi.org/10.3390/horticulturae5020041.

[18] F.A. Simão, R.M. Waterhouse, P. Ioannidis, E.V. Kriventseva, E.M. Zdobnov, BUSCO: assessing genome assembly and annotation completeness with single-copy orthologs, Bioinformatics 31 (19) (2015) 3210–3212, https://doi.org/10.1093/bioinformatics/btv351.

[19] S. Andrews, FastQC: a quality control tool for high throughput sequence data, Available online at: http://www.bioinformatics.babraham.ac.uk/projects/fastqc, 2010.

[20] A.M. Bolger, M. Lohse, B. Usadel, Trimmomatic: a flexible trimmer for Illumina sequence data, Bioinformatics 30 (15) (2014) 2114–2120, https://doi.org/10.1093/bioinformatics/btu170.

[21] M. Kanehisa, M. Furumichi, Y. Sato, M. Kawashima, M. Ishiguro-Watanabe, KEGG for taxonomy-based analysis of pathways and genomes, Nucleic Acids Res. 51 (D1) (2023) D587–D592, https://doi.org/10.1093/nar/gkac963.

[22] K. Blin, S. Shaw, H.E. Augustijn, Z.L. Reitz, F. Biermann, M. Alanjary, T. Weber, antiSMASH 7.0: New and improved predictions for detection, regulation, chemical structures and visualisation, Nucleic Acids Res. (2023), https://doi.org/10.1093/nar/gkad344.

[23] M.C. Magno-Perez-Bryan, P.M. Martinez-Garcia, J. Hierrezuelo, P. Rodriguez-Palenzuela, E. Arrebola, C. Ramos, D. Romero, Comparative genomics within the *Bacillus* genus reveal the singularities of two robust *Bacillus amyloliquefaciens* biocontrol strains, Mol. Plant Microbe Interact. 28 (10) (2015) 1102–1116, https://doi.org/10.1094/MPMI-02-15-0023-R.

[24] G. Liu, Y. Kong, Y. Fan, C. Geng, D. Peng, M. Sun, Data on genome analysis of *Bacillus velezensis* LS69, 2017 May 5, Data Brief 13 (2017) 1–5, https://doi.org/10.1016/j.dib.2017.04.053. PMID: 28560275; PMCID: PMC5436065.

[25] Y. Yan, W. Xu, W. Chen, Y. Hu, Z. Wang, Complete genome sequence of *Bacillus velezensis* YYC, a bacterium isolated from the tomato rhizosphere, Arch. Microbiol. 204 (2022) 1–5. https://10.1007/s00203-021-02709-5.

[26] L.C. Carvalhais, P.G. Dennis, D.V. Badri, G.W. Tyson, J.M. Vivanco, P.M. Schenk, Activation of the jasmonic acid plant defence pathway alters the composition of rhizosphere bacterial communities, PLoS One 8 (2) (2013) e56457, https://doi.org/10.1371/journal.pone.0056457.

[27] M. Miethke, O. Klotz, U. Linne, J.J. May, C.L. Beckering, M.A. Marahiel, Ferri-bacillibactin uptake and hydrolysis in *Bacillus subtilis*, Mol. Microbiol. 61 (6) (2006) 1413–1427, https://doi.org/10.1111/j.1365-2958.2006.05321.x.

[28] D. Romero, H. Vlamakis, R. Losick, R. Koltera, Functional analysis of the accessory protein TapA in *Bacillus subtilis* amyloid fiber assembly, J. Bacteriol. 196 (2014) 1505–1513, https://doi.org/10.1128/JB.01363-13.

[29] H. Zeriouh, A. de Vicente, A. Pérez-García, D. Romero, Surfactin triggers biofilm formation of *Bacillus subtilis* in melon phylloplane and contributes to the biocontrol activity, Environ. Microbiol. 16 (2014) 2196–2211, https://doi.org/10.1111/1462-2920.12271.

[30] A. Pérez-García, D. Romero, A. de Vicente, Plant protection and growth stimulation by microorganisms: biotechnological applications of bacilli in agriculture, Curr. Opin. Biotechnol. 22 (2011) 187–193, https://doi.org/10.1016/j.copbio.2010.12.003. PMID: 21211960.

[31] H. Feng, N. Zhang, R. Fu, Y. Liu, T. Krell, W. Du, et al., Recognition of dominant attractants by key chemoreceptors mediates recruitment of plant growth-promoting rhizobacteria, Environ. Microbiol. 21 (2019) 402–415, https://doi.org/10.1111/1462-2920.14472. PMID: 30421582.
[32] A. Fessia, R. Ponzio, L. Arcibia, et al., Effects of different light wavelengths on *Bacillus subtilis* and *Bacillus velezensis*, two biocontrol agents isolated from the maize phyllosphere, Arch. Microbiol. 206 (2024) 104, https://doi.org/10.1007/s00203-024-03836-5.
[33] M. Gal, G.M. Preston, R.C. Massey, A.J. Spiers, P.B. Rainey, Genes encoding a cellulosic polymer contribute toward the ecological success of *Pseudomonas fluorescens* SBW25 on plant surfaces, Mol. Ecol. 12 (11) (2003) 3109–3121, https://doi.org/10.1046/j.1365-294x.2003.01953.x. PMID: 14629390.
[34] S.S. Branda, F. Chu, D.B. Kearns, R. Losick, R. Kolter, A major protein component of the *Bacillus subtilis* biofilm matrix, Mol. Microbiol. 59 (2006) 1229–1238, https://doi.org/10.1111/j.1365-2958.2005.05020.x.
[35] H. Vlamakis, Y. Chai, P. Beauregard, R. Losick, R. Kolter, Sticking together: building a biofilm the *Bacillus subtilis* way, Nat. Rev. Microbiol. 11 (3) (2013) 157–168, https://doi.org/10.1038/nrmicro2960. PMCID: PMC3936787.
[36] M.A. Hamon, B.A. Lazazzera, The sporulation transcription factor Spo0A is required for biofilm development in *Bacillus subtilis*, Mol. Microb. 42 (2001) 1199–1209, https://doi.org/10.1046/j.1365-2958.2001.02709.x.
[37] I. Dogsa, K.S. Choudhary, Z. Marsetic, S. Hudaiberdiev, R. Vera, S. Pongor, I. Mandic-Mulec, ComQXPA quorum sensing systems may not be unique to *Bacillus subtilis*: a census in prokaryotic genomes, PLoS One 9 (5) (2014), https://doi.org/10.1371/journal.pone.0096122.
[38] H.E. Na, S. Heo, T. Kim, G. Lee, J.H. Lee, D.W. Jeong, ComQXPA quorum-sensing systems contribute to enhancing the protease activity of *Bacillus velezensis* DMB05 from fermented soybeans, Int. J. Food Microbiol. (2023), https://doi.org/10.1016/j.ijfoodmicro.2023.110294.
[39] F. Gallego del Sol, A. Marina, Structural basis of Rap phosphatase inhibition by Phr peptides, PLoS Biol. 11 (3) (2013) e1001511, https://doi.org/10.1371/journal.pbio.1001511. PMID: 23526880 PMCID: PMC3601957.
[40] G. Gilardi, A. Vasileiadou, A. Garibaldi, M.L. Gullino, Biocontrol agents and resistance inducers reduce phytophthora crown rot (phytophthora capsici) of sweet pepper in closed soilless culture, Phytopathol. Mediterr. 1 (2021) 60, https://doi.org/10.36253/phyto-11978.
[41] M. Ongena, E. Jourdan, A. Adam, M. Paquot, A. Brans, B. Joris, J.L. Arpigny, P. Thonart, Surfactin and fengycin lipopeptides of *Bacillus subtilis* as elicitors of induced systemic resistance in plants, Environ. Microbiol. 9 (2007) 1084–1090, https://doi.org/10.1111/j.1462-2920.2006.01202.x.
[42] A.K. Mukherjee, K. Das, Correlation between diverse cyclic lipopeptides production and regulation of growth and substrate utilization by *Bacillus subtilis* strains in a particular habitat, FEMS Microbiol. Ecol. 54 (3) (2005) 479–489, https://doi.org/10.1016/j.femsec.2005.06.003.
[43] S.P. Chowdhury, J. Uhl, R. Grosch, S. Alquéres, S. Pittroff, K. Dietel, P. Schmitt-Kopplin, R. Borriss, A. Hartmann, Cyclic Lipopeptides of *Bacillus amyloliquefaciens* subsp. plantarum colonizing the lettuce rhizosphere enhance plant defense responses toward the bottom rot pathogen *Rhizoctonia solani*, Mol. Plant Microbe Interact. 28 (9) (2015) 984–995, https://doi.org/10.1094/MPMI-03-15-0066-R. Epub 2015 Aug 28. PMID: 26011557.
[44] N. Zhang, D. Yang, D. Wang, Y. Miao, J. Shao, X. Zhou, et al., Whole transcriptomic analysis of the plant-beneficial *rhizobacterium Bacillus amyloliquefaciens* SQR9 during enhanced biofilm formation regulated by maize root exudates, BMC Genom. 16 (1) (2015) 1–20, https://doi.org/10.1186/s12864-015-1825-5.
[45] X.H. Chen, A. Koumoutsi, R. Scholz, K. Schneider, J. Vater, R. Süssmuth, Genome analysis of *Bacillus amyloliquefaciens* FZB42 reveals its potential for biocontrol of plant pathogens, J. Biotechnol. 140 (2009) 27–37, https://doi.org/10.1016/j.jbiotec.2008.10.011.
[46] J. Palazzini, C.A. Dunlap, M.J. Bowman, S.N. Chulze, *Bacillus velezensis* RC 18 as a biocontrol agent to reduce fusarium head blight and deoxynivalenol accumulation: genome sequencing and secondary metabolite cluster profiles, Microbiol. Res. 192 (2016) 30–36, https://doi.org/10.1016/j.micres.2016.06.002.